Quasi-GPDs from Lattice QCD

Principal Investigator: Martha Constantinou [a],

Project participants: Constantia Alexandrou [b,c], ***Krzysztof Cichy*** [d], ***Kyriakos Hadjiyiannakou*** [c], ***Karl Jansen*** [e], ***Colin Lauer*** [a], ***Aurora Scapellato*** [b,f], ***Fernanda Steffens*** [g]

[a] Temple University,1925 N. 12th Street, Philadelphia, PA 19122-1801, USA
[b] Department of Physics, University of Cyprus, P.O. Box 20537, 1678 Nicosia, Cyprus
[c] Computation-based Science and Technology Research Center, The Cyprus Institute, 20 Kavafi Str., Nicosia 2121, Cyprus
[d] Faculty of Physics, Adam Mickiewicz University, Umultowska 85, 61-614 Poznań, Poland
[e] NIC, DESY, Platanenallee 6, D-15738 Zeuthen, Germany
[f] University of Wuppertal, Gaußstr. 20, 42119 Wuppertal, Germany
[g] Institut für Strahlen- und Kernphysik, Rheinische Friedrich-Wilhelms-Universität Bonn, Nussallee 14-16, 53115 Bonn

Abstract

Understanding hadron structure from first principles is considered a milestone of hadronic physics and numerous theoretical investigations have been devoted to its study. The proposed research focuses on the quantitative description of quark distribution functions within the nucleon. This will be achieved via calculations of generalized parton distributions which complement existing knowledge from PDFs, and are needed for the three dimensional structure of hadrons. We will extract the unpolarized, helicity and transversity GPDs using an N_f=2+1+1 ensemble of twisted mass fermions at a pion mass of about 270 MeV, volume $32^3 \times 64$ and a lattice spacing 0.093 fm. We will explore three values of the nucleon momentum (1.7, 2.1, 2.5 GeV), three values of the source-sink separation (0.75, 0.93, 1.12 fm), and momentum transferred squared up to 2 GeV^2. Within the proposed activities we include the renormalization functions necessary for these quantities. Systematic uncertainties, such as excited states contamination, renormalization and matching formalism will be investigated.

To succeed our scientific goals as described in this proposal we request a total allocation of 12 M Sky-core-hours (BNL/FNAL), 15 TB of disc space (112.5 K Sky-core-hours) and 20 TB (26 K Sky-core-hours) of storage space (BNL/FNAL).

I. INTRODUCTION

The internal properties of hadrons are studied using a set of appropriate quantities, that can be measured experimentally and calculated theoretically. The QCD factorization provides the appropriate formalism and can relate measurements from different processes to *parton distributions*. These are non-perturbative quantities describing the parton dynamics within a hadron, and have the advantage of being universal. The comprehensive study of parton distributions can provide a wealth of information on the hadrons, in terms of variables defined in the longitudinal direction (with respect to the hadron momentum) in momentum space, and two transverse directions. The latter can be defined either in position or momentum space. Parton distributions fall into three categories (PDFs, GPDs, TMDs) based on their dependence on the longitudinal momentum fraction, x, the longitudinal momentum fraction, ξ, the momentum k_T transverse to the hadron direction of motion, and the momentum transferred to the hadron, t. Most of the knowledge on the hadron structure is obtained from DIS and SIDIS data on PDFs, while the GPDs and TMDs are less known. However, even PDFs are not well-determined, as one needs a large number of different processes and targets and a sophisticated setup for polarized beams and targets in the case of the helicity and transversity PDFs. Therefore, calculations from *first principle* are imperative, and the only known approach that captures the full non-perturbative QCD dynamics is Lattice QCD.

Parton distributions are light-cone correlation functions and it is therefore not straightforward to calculate them directly on a Euclidean lattice. Instead, one may calculate their corresponding Mellin moments expressed in terms of hadron matrix elements of local operators, and through the operator product expansion the original light-cone correlation functions can be reconstructed. Realistically, only the lowest moments of PDFs and GPDs can be computed due to large gauge noise in high moments, and also unavoidable power-divergent mixing with lower-dimensional operators.

A recent approach developed by X. Ji [1] has proven that one can access parton distributions via the calculation of correlators of momentum boosted hadrons coupled with non-local spatial operators, that give the so-called quasi-distributions. For large enough momenta, these can be related to the physical (light-cone) distributions via a matching procedure using large momentum effective theory (LaMET). The first investigations led to promising results [2, 3], and recently several theoretical and technical challenges have been clarified and resolved (see Ref. [4] for a recent review on the field of quasi-PDFs), some of them by members of our group, such are the development of a renormalization prescription. Last year we completed calculations of nucleon quasi-PDFs with simulations at the physical point and extracted the unpolarized, helicity and transversity PDFs [5, 6].

II. PROPOSED ACTIVITIES - ANTICIPATED RESULTS

With this request for computer allocation we propose an extension of our existing research program on quasi-distributions, in order to compute quasi-GPDs which complement TMDs in the study of the three-dimensional structure of hadrons. In particular, we will compute the unpolarized, helicity and transversity quasi-GPDs of the nucleon with momentum transferred squared, Q^2, up to $\sim$2 GeV^2. The proposed study is among the first for quasi-GPDs, and significant knowledge needs to be acquired prior proposing simulations at the physical point. The overall setup must be optimized, so that future state-of-the-art calculations make optimal use of the limited computational resources available to the lattice community. Therefore, we will consider the connected contributions to nucleon quasi-GPDs for an ensemble of gauge configurations simulated with two light degenerate quarks, a strange and a charm quark in the sea (N_f=2+1+1) and a pion mass of about 270 MeV. This will keep the computational cost within reach. We will employ the twisted mass & clover formulation [7] and Iwasaki improved gluonic action. The parameters are listed in Table I below.

The quasi-distribution approach requires matrix elements with fast moving hadrons, and we will use three values for the momentum boost: $8\pi/L$, $10\pi/L$ and $12\pi/L$, corresponding in physical units to 1.7, 2.1 and 2.5 GeV. Since several momentum-transfer vectors lead to the same value of Q^2, we will compute the relevant matrix elements for $\mathcal{O}(50)$ choices of such vectors (for $Q^2 \leq 2$ GeV^2), allowing also to average over the equivalent choices. After optimizing the setup, we will investigate the choice of Q-vectors to identify if some lead to reasonable signal-to-noise ratios at the given nucleon boost. Study of systematic uncertainties is crucial for reliable extraction of estimates. In this work we will study excited states contamination which can be done with a single ensemble. We will produce data at source sink separation $T_{\rm sink}/a$=8, 10, 12 which corresponds to 0.75, 0.93, 1.12 fm. In addition, the results from this work will be a basis to investigate other systematics (finite lattice spacing, finite volume, non-physical pion mass, etc) in the near future, to obtain GPDs from first principles formalism, with fully quantified uncertainties.

To extract light-cone GPDs using the quasi-GPDs approach requires, among others, an appropriate renormalization program and a matching formalism within LaMET. We will use the RI$'$-type renormalization scheme that we developed in Refs. [8, 9], to obtain the renormalization functions non-perturbatively. Apart from using the available matching formulae for the unpolarized case [10], bringing the RI-renormalized quasi-GPDs to $\overline{\rm MS}$-renormalized light-cone GPDs, we will derive formulae for the matching of $\overline{\rm MS}$ quasi-GPDs to $\overline{\rm MS}$ GPDs for all Dirac structures.

In a nutshell, the anticipated results are:

• Martix elements for vector, axial and tensor non-local operators containing a straight Wilson line for momentum boost 1.7, 2.1, 2.5 GeV and momentum transfer squared up to 2 GeV^2. The three values of the source-sink separation that will be employed for study of excited states contamination are 0.75, 0.93, 1.12 fm.

• Renormalization functions for the three types of GPDs. We will compute the Z-factors using N_f=4 ensembles at five values pion masses (350 - 550 MeV) and take the chiral limit. These N_f=4 configurations have been already provided to our group

• Study of excited states contamination

• Final estimates on light-cone GPDs (unpolarized, helicity and transversity) using the matching formulas between $\overline{\rm MS}$ quasi-GPDs and $\overline{\rm MS}$ GPDs for all Dirac structures

This project brings together researchers from US and European Institutions, and utilizes their wide range of expertise. The latter covers all aspects needed for the numerical calculations proposed here (theoretical developments, algorithmic development, data production, renormalization, data analysis, physical interpretation), which guarantees a smooth progress of the activities. All members are part of the former European Twisted Mass Collaboration which has officially changed its name to **Extended Twisted Mass Collaboration**, as it comprises now members also from US Institutions. Such an international collaboration has high value as we have immediate access to state-of-the-art configurations. The Extended Twisted Mass Collaboration has produced a $64^3\times128$ ensemble at the physical point with volume ∼5.2 fm, and is currently producing two ensembles at similar volume: $80^3\times160$ with a=0.07 fm and $96^3\times192$ with a=0.055 fm. These three ensembles will enable a continuum limit at the physical point. In the near future, these ensembles will be used for the activities we propose here. We note that part of the proposed activities is funded by the US National Science Foundation (Grant No. PHY-1714407). Therefore, it is natural to seek for support from US computational resources.

The proposed calculations align with the scientific goals of USQCD Collaboration on hadron structure, as stated in the recent "Hadrons and Nuclei" whitepaper. They will also contribute to the strategic plan of both USQCD and DOE:

- Understanding the internal quark-gluon structure of hadrons from first principles remains a long-term goal of Nuclear Physics, and has been emphasized, e.g., in the Nuclear Science Advisory Committee's Long Range Plan (LRP2015) [11]. A future electron-ion collider (EIC) has been identified as the "highest priority for new facility construction" by the 2015 Nuclear Science Advisory Committee's Long Range plan [11]. Recently, the National Academies of Sciences, Engineering, and Medicine (NAS) strongly endorsed the science case for an EIC in their assessment report [12]. The proposed activities are in accordance with the physics goal of the EIC which includes the 3-D structure of hadrons. Acquiring USQCD resources will enable US leadership in electron-ion collider (EIC) science.
- Acquiring access to the requested resources will allow us, not only to obtain state-of-the-art lattice results, but also optimize our algorithms in preparation for the exascale supercomputing era. The latter is among the six pillars of DOE's mission, aiming at "generating the greatest possible intellectual and economic benefit". To this end, we will engagement young researchers in forefront fundamental research and HPC, ensuring their further development and emergence as independent researchers, establishing US leadership in advance computing research.

III. THEORETICAL AND COMPUTATIONAL APPROACH

GPDs can be accessed in lattice QCD using a similar principle as used in the quasi-distribution approach for PDFs, i.e. computing matrix elements probing spatial, instead of light-cone correlations. In this way, quasi-GPDs are obtained, which can be matched to their light-cone counterparts via LaMET. The object computed on the lattice is:

$$\tilde{q}^{\Gamma}_{\rm GPD}(x,\xi,t,P^3,\mu) = \int \frac{dz}{4\pi} e^{ixP^3 z} \langle P''|\bar{\psi}\,(0)\,\Gamma\lambda^a W_3(0,z)\psi\left(\frac{z}{2}\right)|P'\rangle\,, \tag{1}$$

where P_3 – momentum boost in the longitudinal direction (taken to be the 3-direction), $W_3(0,z)$ – Wilson line of length z along the boost direction, $|P'\rangle$ ($|P''\rangle$) is the initial (final) state labeled by its momentum, μ – renormalization scale (in some chosen scheme), x – momentum fraction of the parton, $t=Q^2$ is the momentum transfer squared (P'+Q=P'') and ξ is the quasi-skewness variable, defined as $\xi = -\frac{P''^3-P'^3}{P''^3+P'^3} = -\frac{Q^3}{2P^3}$ (equal to the light-cone skewness variable up to power-suppressed corrections in $1/P_3^2$). The Dirac structure Γ determines the type of quasi-GPD that can be accessed and different choices correspond to unpolarized, helicity and transversity quasi-GPDs. For unpolarized GPDs, we will use Γ=γ^0 (instead of γ^3 which is parallel to the direction of the Wilson line) because it avoids mixing with a twist-3 operator for non-chirally symmetric lattice actions [8]. Eq. (1) shows that the calculated matrix element is the same one as computed for quasi-PDFs, but with momentum transfer inserted in the operator. Obviously, for Q^2=0 Eq. (1) becomes the definition of the quasi-PDFs. The quasi-GPDs are generalized form factors of the object computed in Eq. (1). We write as an example, the decomposition for chiral-even unpolarized and helicity GPDs:

$$\tilde{q}^{\Gamma}_{\rm GPD}(x,\xi,t,P^3,\mu) = \bar{u}(P'')\left\{\tilde{H}^{\Gamma}(x,\xi,t,P^3,\mu)\Gamma + \tilde{E}^{\Gamma}(x,\xi,t,P^3,\mu)\frac{[\not{\Delta},\Gamma]}{4M}\right\}u(P')\,, \tag{2}$$

where $\tilde{H}$ and $\tilde{E}$ are referred to as quasi-GPDs and M is the nucleon mass. In the chiral-odd transversity case, there are two additional form factors.

A crucial aspect of the calculation is the renormalization, which removes divergences with respect to the regulator. The renormalization of quasi-distribution is far from trivial, as the presence of the Wilson line brings in additional divergences, (power-law) and prohibit one to take the continuum limit. In 2017 we proposed for the first time [13] a non-perturbative renormalization prescription which was formulated based on understanding the renormalization pattern of our work within lattice perturbation theory [8]. The latter work revealed an unknown feature of the non-local bilinear operators containing a Wilson line: a mixing between the vector operator when the Dirac structure is in the same direction as the Wilson line. We employed the non-perturbative prescription in Ref. [9] for the first time, and the prescription (including variations) has been implemented by all calculations of quasi-distributions (see, e.g., Refs. [5, 6, 14–18]). Furthermore, our perturbative calculation has changed the landscape of the numerical simulations, as an alternative operator is now used for the unpolarized distributions (γ^0).

We will employ the RI$'$ scheme for the renormalization of quasi-GPDs, which a mass-independent scheme and an extrapolation to the chiral limit is needed. Since the ensemble used is N_f=2+1+1, a proper determination of the renormalization functions requires dedicated simulations on ensembles with all flavor quarks degenerate N_f=4. In addition, their coupling constant must correspond to the same value of the coupling constants as the N_f=2+1+1 ensembles used for the calculation of quasi-GPDs. Such ensembles have been produced and are available to our group. We will use 5 ensembles corresponding to pion mass in the range [350 - 550] MeV (am_{PS}=0.1680(5), 0.1916(8), 0.2129(8), 0.2293(7), 0.2432(6)) and we will take the chiral limit. Several values of the RI$'$ scale, μ_0, will be employed for each ensemble in order to take the $(a\mu_0)^2\to0$ limit upon conversion to the MS and at a common scale. This will eliminate residual dependence on the initial RI$'$ scale, and give more reliable estimates for the renormalization functions. In our renormalization program we will use 15 choices for the scale in the range $(a\mu_0)^2\,\epsilon\,[1-5]$. The computational approach relies on momentum sources that offers high statistical accuracy with a small statistical sample ($\mathcal{O}(10)$).

The renormalized quasi-GPDs can be related to light-cone GPDs through a factorization formula:

$$\tilde{G}^\Gamma(x,\xi,t,P^3,\mu) = \int_{-1}^{1}\frac{dy}{|y|}\,C_G^\Gamma\left(\frac{x}{y},\frac{\xi}{y},\frac{\mu}{yP^3}\right)G^\Gamma(y,\xi,t,\mu) + \mathcal{O}\left(\frac{M^2}{P_z^3},\frac{\Lambda^2_{\rm QCD}}{P_3^2}\right), \qquad (3)$$

where $\tilde{G}$ is any of the form factors and C_G^Γ is the perturbatively computed matching kernel, for a given type of GPD and its related Dirac structure. This formula establishes that quasi-GPDs are equal to light-cone GPDs up to power-suppressed corrections (nucleon mass corrections and higher-twist corrections). The matching coefficient was first derived for flavor non-singlet unpolarized and helicity quasi-GPDs in Ref. [19] and for transversity quasi-GPDs in Ref. [20], using the transverse momentum cutoff scheme. Recently, a matching formula for the unpolarized case was also derived [10], relating quasi-GPDs renormalized in a variant of the RI/MOM scheme to $\overline{\rm MS}$ light-cone PDFs. We also note that quasi-GPDs $\tilde{H}$ reduce to quasi-PDFs for ξ=t=0, while $\tilde{E}$, or the additional two form factors in the transversity case, have no quasi-PDF counterparts. The x-integrals of GPDs obtained after applying the matching procedure give different kinds of form factors that can be computed on the lattice with standard methods, e.g. the Dirac and Pauli form factors $F_1(t), F_2(t)$ in the unpolarized case and the generalized axial and pseudoscalar form factors $G_A(t), G_P(t)$ for helicity.

In the proposed activities, we will compute the flavor non-singlet $(u-d)$ nucleon matrix elements defining $\tilde{q}^\Gamma_{\rm GPD}$ for three types of Dirac structure, corresponding to the unpolarized, helicity and transversity cases (twist-2). The isovector flavor combination receives only contributions from the connected diagram, which keeps the required computational resources at a reasonable cost. In the exploratory phase, we will investigate the quality of the signal for different nucleon boosts P_3 and momentum transfers Q. The signal-to-noise ratio decreases when the magnitude of P_3 and Q increases and moreover, a necessary condition to obtain reliable results is to ensure ground state dominance. The latter requires to keep the source-sink separation, $T_{\rm sink}$, large enough, to have good control over the excited states and obtain results that effectively describe the properties of the nucleon ground state. The interplay of the magnitude of momenta P_3, Q and the source-sink separation will be investigated in detail. Our extensive prior experience indicates that, for the intended ensemble (at pion mass of 270 MeV) and at Q^2=0, nucleon boosts up to 2.5 GeV can be reliably reached, i.e. with $T_{\rm sink}$ values such that at least the largest one is above 1 fm (and yields good precision, with relative errors below $\mathcal{O}(10)\,\%$) and ground state dominance can be shown by comparing different analysis techniques (single-state, two-state fits, summation method). We expect that at increasing Q^2, the maximum reachable P_3 will be smaller and it is an important aim of the project to analyze the feasibility of reaching large momentum transfers at large nucleon boosts, to cover a wide kinematic range of quasi- and light-cone GPDs.

We will use momentum smeared interpolating fields in the correlators to improve overlap with a boosted nucleon, resulting in a large reduction in the statistical errors as explained in Section V B. To evaluate the three-point functions, we will compute the all-to-all propagator by using the sequential method at fixed source-sink separation. This approach is advantageous when combined with the momentum smearing technique, as discussed in Ref. [21].

We will employ the twisted mass (TM) formulation [7] with a clover term for the discretization of the fermion action, and Iwasaki-improved gluon action. The major advantage of TM fermions is an automatic $\mathcal{O}(a)$-improvement of all physical observables (a: lattice spacing), achieved by tuning the bare untwisted quark mass to its critical value m_{cr}, during generation of the configurations with no further operator improvement required [22]. In practice, maximal twist of Wilson quarks is implemented by tuning m_0 to zero, while the twisted quark mass parameter μ is kept non-vanishing to give a mass to the hadrons. The gauge configurations of twisted mass & clover (see Table I) have already been produced by the Extended Twisted Mass Collaboration.

Ensemble	lattice spacing a	Volume ($L^3 \times T$)	m_π (MeV)	$m_\pi\, L$
cA211.32	0.093 fm	$32^3 \times 64$	270	4

TABLE I: Twisted mass ensemble with a clover term that will be used in the proposed activities.

The PI has long-standing experience with TM fermions which guarantees the successful implementation of the project. The suitability of the TM formulation has been extensively demonstrated by the work of the group, and in particular with recent results obtained by our group on moments of PDFs using physical pion mass ensembles. This includes results for nucleon matrix elements of the ultra-local and first derivative operators [23], a calculation of nucleon σ-terms to unprecedented accuracy [24], a pioneering calculation of the proton spin [25], and quasi-PDFs at the physical point [5, 6].

IV. LATTICE FORMULATION AND EXISTING EXPERTISE

Our group has extensive experience in computation of hadron structure and in nucleon quasi-PDFs and studies of their systematic uncertainties [5, 6, 8, 9, 21, 26] and hadron structure in general. Our most recent work is on an ensemble at the physical point using N_f=2 twisted mass fermions, for the computation of all three types of PDFs (unpolarized, helicity and transversity) using the quasi-PDFs approach. We have used three values of the nucleon momentum, namely 0.83 GeV, 1.1 GeV and 1.4 GeV, and multiple source-sink separations.

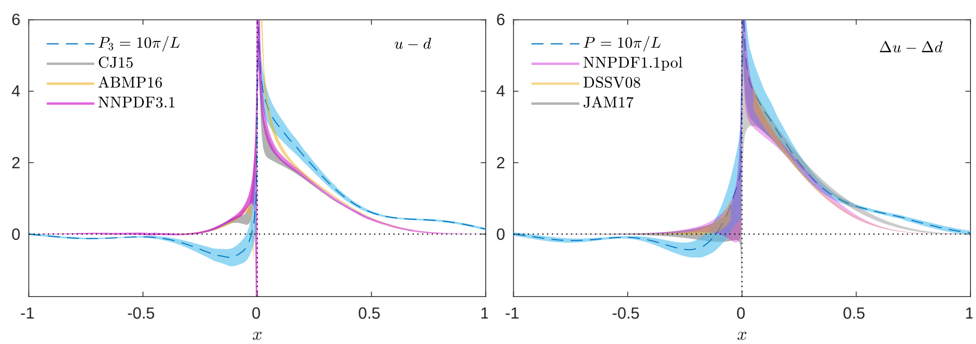

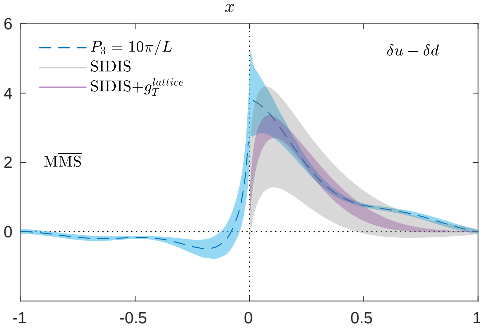

FIG. 1: Final results for the unpolarized PDF (upper left), helicity PDF (upper right) and transversity PDF (lower), using the largest momentum P_3=$10\pi/L$ (blue curve). The global fits of Refs. [27–29] (unpolarized), Refs. [30–32] (helicity), Refs. [33] (transversity) are shown for qualitative comparison.

The lattice results at the highest momentum are shown in Fig. 1 together with phenomenological fits for qualitative comparison. The unpolarized and helicity PDFs approach the phenomenologically determined curves showing encouraging results. For the helicity there is a better agreement for a large range of Bjorken-x values. The unphysical oscillations, more severe in the antiquark region (negative x) find their origin at the slow decay of the matrix elements to zero for large z values. The effect is naturally suppressed for larger nucleon boosts, for which matrix elements decay to zero fast enough. The case of the transversity is particularly interesting, as it is very poorly constrained from semi-inclusive scattering processes (SIDIS), and lattice QCD can provide a determination with higher accuracy, as can be seen in Fig. 1 (lower panel). Our results show that after applying the renormalization, matching procedure [5] and Target Mass Corrections (TMCs) [34], PDFs extracted in lattice QCD approach the phenomenological PDFs as the boost increases. This demonstrates the applicability of the quasi-PDFs approach and the success of the renormalization procedure developed by our group.

In the aforementioned work [26] we refined our renormalization program and we performed a chiral extrapolation on 5 ensembles with different value of the pion mass. We employed 13 values of the RI′ renormalization scale, μ_0, in order to eliminate residual dependence on μ_0 in the $\overline{\text{MS}}$-scheme estimates at 2 GeV, via a fit $(a\mu_0)^2\rightarrow 0$.

The expertise gained by the study of quasi-PDFs will be utilized for nucleon quasi-GPDs, and we extended all our algorithms for quasi-PDFs to include momentum transfer between the initial and final states. We completed the necessary preparatory work, which supports directly the proposed research, with all codes for the quantities of interest developed, cross-checked, compiled on different architectures and first data have been produced for a test ensemble with smaller volume.

A. Relevant effort by other lattice groups

As for many other quantities calculated within lattice QCD, there are several independent efforts to extract x-dependent distribution functions by other groups within and outside USQCD. This includes other groups investigating nucleon and pion quasi-distributions (LP^3, BNL group) pseudo-distributions (William & Mary / JLab group), good lattice cross sections (JLab group), auxiliary heavy quark field formalism (MIT group), hadronic tensor (χQCD), OPE without OPE (UKQCD/QCDSF), auxiliary light quark filed formalism (RQCD) (for a summary see, e.g., the recent review of Ref. [4]). The work of each lattice group is unique in the employed approach, lattice formulation, simulation parameters and analysis methods. Knowledge from different formalisms, technical approach, and analysis methodologies is highly desirable, as each calculation may suffers from different systematic uncertainties. Understanding ones systematics is crucial for improving the next generation of calculations.

Our group complements the efforts of the scientific community, and has been leading some aspects for quasi-PDFs, with more prominent ones the development of the renormalization prescription and the application of momentum smearing [35], and demonstrated the reduction of gauge noise. The latter was instrumental for simulations at the physical point. Our strategic plan is to continue calculations exploring new techniques, algorithmic improvement, and refined analysis methods. This line of research has led to a series of published papers in high-impact peer-reviewed Journals for quasi-PDFs. We have recently prepared an extensive article [26] on thorough investigation of uncertainties for quasi-PDFs at the physical point targeted to the Lattice community. In this work we clearly demonstrate, among others, the effect for several sources of systematic uncertainties. With the proposed activities we intend to continue contributing to the progress in x-dependent distribution functions.

V. COMPUTATIONAL TECHNIQUES - CODE PERFORMANCE

Our ability to carry out simulations with parameters at or close to their physical values is due to the synergy of increase of computational resources, and algorithmic improvements. Of particular interest to the current proposal is the development and tuning of the multigrid algorithm for twisted mass fermions.

A. DD-αAMG for twisted mass operator

The multi-grid approach was extended to solve two non-degenerate flavors (1+1) that arise in the strange-charm sector. This has been already tuned by our group and, thus, it is production-ready. We demonstrate the efficiency of our algorithms using our CPU implementations where both ARPACK-CG (implementation of eigenvalue deflation in the Conjugate Gradient code) and multi-grid are tested and can be compared directly. The implementation of multi-grid has led to impressive reduction of the computational cost, as demonstrated in Fig. 2, which shows the speedup achieved for both ARPACK-CG and multi-grid with respect to CG.

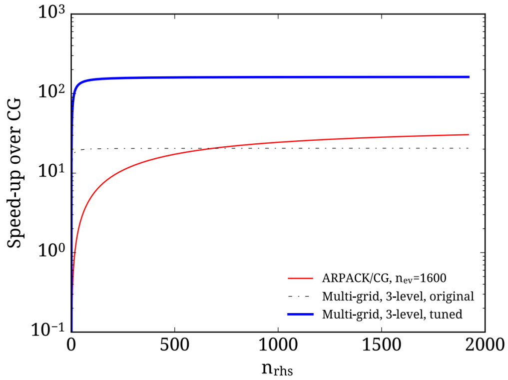

FIG. 2: Speedup of ARPACK-CG and multi-grid over CG in core-hours as a function of the accumulated rhs. We show ARPACK-CG (red curve), multi-grid with the parameters tuned for clover fermions [36] (dashed curve) and multi-grid with parameters we optimized for twisted mass fermions (blue curve).

We have tuned the parameters for the multi-grid algorithm achieving an additional three-fold speedup compared to the originally proposed multi-grid for clover fermions [36].

In DD-αAMG, a flexible iterative Krylov solver is preconditioned at every iteration step by a multi-grid approach [36] given by the error propagation, $\epsilon \leftarrow (I - MD)^k(I - PD_c^{-1}P^\dagger D)\epsilon$, where M is the smoother, k are the number of smoothing iterations, P is the prolongation operator and $D_c = P^\dagger DP$ is the coarse grid operator. The multi-grid preconditioner exploits domain decomposition strategies having as a smoother the Schwarz Alternating Procedure (SAP) [37] and as a coarse grid correction an aggregation-based coarse grid operator. The method is designed to deal efficiently with both infrared (IR)- and ultra-violet (UV)-modes of D. Indeed, the smoother reduces the error components belong- ing to the UV-modes [36], while the coarse grid correction deals with the IR-modes. This is achieved by using an interpolation operator P , which approximately spans the eigenspace of the small eigenvalues. Thanks to the property of local coherence [38] the subspace can be approximated by aggregating over a small set of $N_v \sim \mathcal{O}(20)$ test vectors v_i, which are computed in DD-αAMG via an adaptive setup phase [36]. In Ref. [39] we have extended the DD-αAMG approach to the degenerate twisted mass operator $D(\pm\mu) = D_W \pm i\Gamma_5\mu$ showing a speed-up of two orders of magnitude at the physical point compared to the conjugate gradient method (CG). As depicted in Fig. 3 the speed-up is greater the smaller the pion mass.

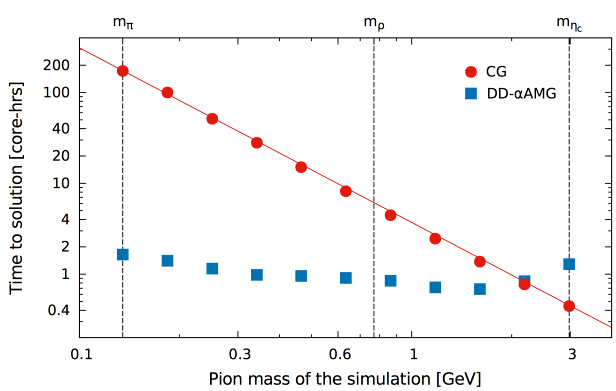

FIG. 3: Time to invert one right-hand- side, in core-hours, as a function of the pion mass. We compare the standard Conjugate Gradient (CG) to our multi-grid implementation (DD-αAMG). We see that critical slowing down is drastically improved when using DD-αAMG as we approach the physical point. The results are for mixed precision odd-even preconditioned CG and three-level DD-αAMG using a $48^3 \times 96$ lattice.

We also note that the memory requirements of the multi-grid algorithm are significantly reduced compared to our ARPACK/CG algorithm, since keeping a large number of a few hundred eigenvectors in memory is not required.

B. Momentum smearing

The momentum smearing technique was proposed in Ref. [35] and is extremely advantageous when matrix elements of boosted states are being computed in lattice QCD by improving the overlap with the ground state of the boosted particle. It is a modification of the Gaussian smearing function [40, 41], applied to the quark fields. We have successfully applied this method in our exploratory study of PDFs carried out using an ensemble with a higher pion mass [21] and found that we needed a factor of 200 less statistics to obtain the same statistical errors, at boost $6\pi/L \sim 1.41$ GeV and $T_{\rm sink}$=$8a \sim 0.65$ fm, as compared to only Gaussian smearing. This is shown in Fig. 4 for the real part of the matrix elements for the unpolarized $u - d$ distribution.

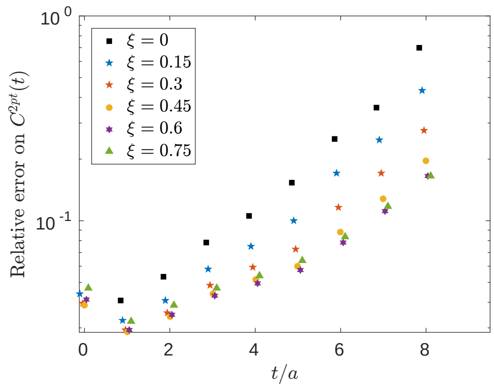

FIG. 4: Right: Relative error on the nucleon two-point correlation function for the cA2.48 ensemble as a function of the source-sink separation for different values of the momentum smearing parameter ξ. The points at $\xi = 0$ (black squares) refer to the case of only Gaussian smearing applied.

The drawback of momentum smearing is that new inversions of the Dirac operator are required for each momentum. The momentum smearing function contains a free parameter ξ that has to be tuned in order to maximize the overlap of the interpolating fields with the ground state of the boosted particle. In Fig. 4 we show an example of the tuning procedure carried out for 50 measurements for the nucleon two-point function, for a momentum p=$8\pi/L \sim 1.11$ GeV. As can be seen, the relative error on the two-point function increases exponentially with the time separation t_s, but it is drastically reduced when $\xi \in [0.6 - 0.75]$ as compared to ξ=0, which corresponds to only Gaussian smearing. Therefore before we start production runs, we will tune the momentum smearing parameter for each value of the momentum used in PDFs calculation.

C. Multiple measurements per configuration

For two- and three-point functions, the large number of statistics needed is obtained by calculating correlation functions from different source-positions on the same configuration. This is how we take advantage of the large speedups from multi-grid, since for every source-position a new set of quark propagators are produced. On a large enough lattice, and given that the source-positions are selected randomly, the auto-correlations become very small, and data on multiple source-positions on the same configuration can be considered statistically independent.

We find that that the statistical error of various quantities drops with the inverse square root of the number of source-positions, which indicates uncorrelated data. Also, for a given number of measurements, N_{meas}, we have analyzed data from only 1 source-position for N_{conf}=N_{meas}, as well as, 16 source-positions for N_{conf}=$\frac{N_{meas}}{16}$. The scaling of the error was the same between those two sets. Given the large speed-up achieved with the use of the multi-grid and multiple right-hand-side an efficient increase in statistics is achieved by computing correlation functions from different source-positions on the same configuration.

VI. EFFICIENT USE OF COMPUTATIONAL RESOURCES

Even though no further code development is needed, we will continue investigating algorithmic improvements and computational techniques in the course of this project, along several directions. This includes opportunities for faster calculation of quark propagators using multi-grid, more efficient usage of data management and analysis tools.

The computation of quark propagators is the most demanding component of the project and requires the implementation of the most efficient algorithms. We will use a recently developed deflation algorithm for twisted mass fermions that is highly improved and more than 20 times faster at the physical point as compared to the standard conjugate gradient algorithm. Propagators are contracted appropriately to yield the desired physical observables, and although the contractions are less computationally demanding than the propagator production, they are demanding on memory access latency and bandwidth.

The inverter we will employ uses FGMRES as the outer Krylov subspace solver and a 3-level multigrid preconditioner. This technique requires a set-up phase that constructs prolongator and restrictor vectors used to transpose the original matrix (fine grid) to a matrix with high frequency UV modes filtered out, leaving the difficult low frequency IR modes (coarse grid). This fine-to-coarse preconditioning is done twice. This set-up must be performed once per matrix, then all subsequent inversions performed on that matrix use the same multigrid set-up.

VII. COMPUTATIONAL RESOURCES REQUEST - JUSTIFICATION

We request computer time and storage for the three lattice components for the quasi-GPDs calculation: the two- and three-point functions, and the renormalization functions, as given below:

A. The *two- and three-point functions* will be produce within the same work-flow which reduces the computational cost and the need to save the propagators. The desirable architecture is Skylake CPUs, which is similar to the architecture we used for quasi-PDFs. However, we are able to also migrate our codes to the KNL cluster at JLab. The code has been benchmarked using the ensemble given in Table I, at Okeanos system in Warsaw Supercomputing center[1]. in which each node has 24 Intel Xeon CPU cores (x86_64 architecture, Haswell[2]). In Fig. 5 we report the scaling of the application for a full production run, using 64, 128 and 256 cores.

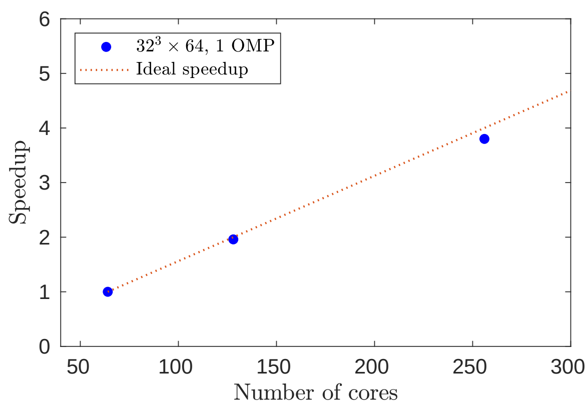

FIG. 5: Scaling of the code for a full production run on the ensemble with lattice volume $32^3\times32$, performed on Okeanos system in Warsaw Supercomputing center with Intel Xeon CPU cores (x86_64 architecture, Haswell). The dashed line shows perfect scaling, while the blue points the real speedup.

As can be seen, the code scales close to the ideal scenario. For number of cores larger than 256 the slight degradation is an expected behavior due to the increased of communications time among the different nodes. Thus, the timings reported in Table II will be based on a setup with 256 cores. Note that, since each node has 24 cores, in Table II we report the cost with the effective number of cores involved in the run, i.e. 264 (11 nodes).

Component	Instances	Wall Clock (hrs)	Cores	Total Core-hrs
Multigrid Set-Up	1	0.0194	264	5.122
Forward Inv. (u)	72	0.09	264	23.760
Forward Inv. (d)	72	0.09	264	23.760
Sequential Inv. (u)	216	0.27	264	71.280
Sequential Inv. (d)	216	0.27	264	71.280
Contractions	120	0.10	264	26.400
Miscellanea		0.032	264	8.448
Total				ESTIMATE: 221.602

TABLE II: Components of the calculation, with the corresponding timings and CPU-hrs based on 264 cores. In the 2nd column we report the number of forward, sequential inversions for both up and down quarks, contractions and other requirements. In the last column, we give the core-hr for each component of the code and final estimate.

Our measurements will be obtained using multiple random source positions per gauge configuration. We aim at 16 source positions, which was the setup used for our calculation of nucleon quasi-PDFs calculation. At a given value of the momentum, $p{=}n\cdot2\pi/L$, we will compute matrix elements with a nucleon boosted along different spatial directions and orientations $(\pm x, \pm y, \pm z)$, which allows one to average over the obtained correlators, reducing further the statistical uncertainties. However, separate inversions of the Dirac operator are required because the momentum

[1] http://kdm.icm.edu.pl/kdm/Okeanos
[2] We note that the reported difference in the performance between Haswell and Skylake is small (5%-10%) so it is not taken into account.

smearing parameter has to be aligned to the direction of the boosts for an optimal overlap of the interpolating field with the boosted particle. The matrix elements will be computed applying link-smearing to the Wilson line in the inserted operator and the results will be saved for only three levels of smearing. This will not affect the number of inversions that have to be carried out, but only the number of contractions among quark propagators. However, as reported in Table II, the contractions have a cost of around 5.5% of the total, in our optimized setup. Each inversion of the Dirac matrix requires 4.5s or 0.33 CPU-hrs when 264 cores are effectively used. Thus, the production of each quark propagator needs 12 × 0.33 CPU-hr=3.96 CPU-hr. Each contraction of quark propagators requires 0.22 CPU-hr. The number of inversions to compute forward propagators, for a fixed quark flavor (up/down), is $3_{col} \times 4_{spin} \times 6_{dir}$=72, requiring 23.76 CPU-hrs, as reported in Table II. To evaluate the unpolarized, helicity, and transversity quasi-GPDs, separate inversions are needed since different projectors enter the sequential source before the inversions are carried out. Thus, the total number of the sequential inversions for a fixed quark flavor insertion (up/down) is $3_{proj} \times 3_{col} \times 4_{spin} \times 6_{dir} = 216$ at a given value of the nucleon boost p. These require a total of 71.28 CPU-hrs. Once computed the forward and sequential propagators, the contractions amount to $6_{dir} \times 2_{up/down} = 12$ for the two-point functions and $6_{dir} \times 2_{up/down} \times 3_{proj} \times 3_{smear} = 108$ for the three-point functions, for a total of 120 contractions. The last two components of the calculation listed in Table II include: 1) Multigrid Set-up for the solver, which is performed only once for each run and takes 5.122 CPU-hrs; 2) Quark and gauge smearings and I/O, that we refer to as Misellanea, which require a total of 8.448 CPU-hrs.

Based on the above, a run on CPU processors requires 221.602 CPU-hours for one $T_{\rm sink}$, one source position on each configuration and with a single momentum boost. We will analyze on average[3] 350 configurations, three values of the nucleon momentum and three values of $T_{\rm sink}$. This brings the total CPU cost for the two- and three-point functions to approximately 11.2M Sky-core-hours.

B. Within the project we intend to calculate the necessary *renormalization functions* for the quasi-GPDs, which has smaller computational cost. For the necessary vertex functions, we need 12 inversions for each configurations and this requires: 12*0.33 CPU-hrs=3.96 CPU-hrs. The total time is dominated by the contractions, that is $3_{dir} \times 3_{smear} \times 0.81 \mathrm{CPU-hrs} = 7.26$ CPU-hrs. The total request will be for 25 configurations, on 5 ensembles and 15 values of the RI′ scale, that is $7.26 \mathrm{CPU-hrs} \times 20_{confs} \times 5_{ensembles} \times 15_{scales}$ ∼14K CPU-hours. We request 14K Sky-core-hours to extract the renormalization functions.

C. The request in *storage* is justified as follows: For each $32^3 \times 64$ configuration, around 250 MB of data are written for the two- (three-) point functions, for the three values of $T_{\rm sink}$, source position, stout smearing and momentum boost. This brings the total storage requirement to $250\mathrm{MB} \times 16_{src.\,pos} \times 3_{smear} \times 3_{boost} \times 350_{confs}$ ∼13 TB. These data are processed to average over the 16 source positions and to create the isovector combination, which adds approximately another 3 TB. Furthermore, the gauge configurations have size 1.2 GB and the total need is ∼ 0.5 TB. Every 100 - 150 configurations we will transfer the data from the scratch to the archival storage, and thus, we require 15 TB of disc space and 20 TB of tape storage, which is equivalent to 112.5 K Sky-core-hrs of disc space and 26 K Sky-core-hrs of tape storage.

To summarize, we request a total of 12 M Sky-core-hours, 15 TB of disc space and 20 TB of tape storage.

VIII. COMPUTATIONAL READINESS - PLAN - MILESTONES

We have done the necessary preparatory work so that we are ready for production within the first two weeks of acquiring the allocation. All the software needed for the computations of the quasi-GPDs have been developed, cross-checked and tested. In addition all the gauge ensembles have been produced and were provided to our group. The analyses codes are currently being generalized to handle the momentum transfer, and we will utilize our existing experience in form factors and generalized form factors.

We intend to start from the smallest value of the momentum boost (1.7 GeV) and we will run in parallel all three types of GPDs (unpolarized, helicity and transversity), and all $T_{\rm sink}$ values. These data will be produced and analyzed within the first quarter of the allocation, and we will assess the signal-to-noise ratio, and excited states contamination. Then we will proceed with momentum 2.1 GeV (second - third quarter), and finally produce the data for the largest

[3] see Section VIII for an exact breakdown

momentum 2.5 GeV (third - forth quarter). We plan to analyze on average 350 gauge configurations with 16 source-positions per configuration. The exact number os configurations depends on the value of $T_{\rm sink}$ and momentum boost, as increasing their values, decreases the signal-to-noise ratio. Our computational plan includes:

- P_3=1.7GeV: 100, 200, 300 configurations for $T_{\rm sink}/a$=8, 10, 12, respectively;
- P_3=2.1 GeV: 200, 350, 500 configurations for $T_{\rm sink}/a$=8, 10, 12, respectively;
- P_3=2.5 GeV: 300, 500, 700 configurations for $T_{\rm sink}/a$=8, 10, 12, respectively,

in order to keep the statistical uncertainties similar between all data. This is crucial for a proper study of systematic uncertainties, for example, an unbiased two-state fit. Since it is impossible for one to know the exact scaling of the statistical error with increase of P_3 and $T_{\rm sink}$, we will fine tune the above numbers once we perform the first analyses.

Each gauge configuration is an independent calculation and can be scheduled separately. We will analyze our statistics in batches depending on the observable, as the project progresses. We list the scientific milestones of the project below, and the timeline for the various tasks in Table III

Quarter	Usage (CPU-hrs)	P_3
1	2 M	1.6 GeV
2	3 M	2.1 GeV
3	4 M	2.1, 2.5 GeV
4	3 M	2.5 GeV

TABLE III: Quarterly computational plan.

M1. First analysis for all quasi-GPDs at P_3=1.7GeV (Month 2)
M2. Final results for all quasi-GPDs at P_3=1.7GeV (Month 4)
M3. Final results for all quasi-GPDs at P_3=2.1GeV (Month 7)
M4. First results for all quasi-GPDs at P_3=2.5GeV (Month 9)
M5. Final results for all quasi-GPDs at P_3=2.5GeV (Month 12)

IX. DATA SHARING

The data that will be generated from the proposed activities will be two- and three-point correlation functions that will be stored on the disc and tape requested. To significantly reduce the storage request we will not save the propagators. Correlators that are computed will be saved to disk and tape. The raw data will be available, upon request, to other researchers once they have been analyzed and published.

[1] X. Ji, *Parton Physics on a Euclidean Lattice*, *Phys. Rev. Lett.* **110** (2013) 262002, [arXiv:1305.1539].

[2] H.-W. Lin, J.-W. Chen, S. D. Cohen, and X. Ji, *Flavor Structure of the Nucleon Sea from Lattice QCD*, *Phys. Rev.* **D91** (2015) 054510, [arXiv:1402.1462].

[3] C. Alexandrou, K. Cichy, V. Drach, E. Garcia-Ramos, K. Hadjiyiannakou, K. Jansen, F. Steffens, and C. Wiese, *First results with twisted mass fermions towards the computation of parton distribution functions on the lattice*, *PoS* **LATTICE2014** (2014) 135, [arXiv:1411.0891].

[4] K. Cichy and M. Constantinou, *A guide to light-cone PDFs from Lattice QCD: an overview of approaches, techniques and results*, arXiv:1811.07248.

[5] C. Alexandrou, K. Cichy, M. Constantinou, K. Jansen, A. Scapellato, and F. Steffens, *Light-Cone Parton Distribution Functions from Lattice QCD*, *Phys. Rev. Lett.* **121** (2018), no. 11 112001, [arXiv:1803.02685].

[6] C. Alexandrou, K. Cichy, M. Constantinou, K. Jansen, A. Scapellato, and F. Steffens, *Transversity parton distribution functions from lattice QCD*, *Phys. Rev. D. (Rapid Communication), in production,* (2018) [arXiv:1807.00232].

[7] **Alpha** Collaboration, R. Frezzotti, P. A. Grassi, S. Sint, and P. Weisz, *Lattice QCD with a chirally twisted mass term*, *JHEP* **08** (2001) 058, [hep-lat/0101001].

[8] M. Constantinou and H. Panagopoulos, *Perturbative renormalization of quasi-parton distribution functions*, *Phys. Rev.* **D96** (2017), no. 5 054506, [arXiv:1705.11193].

[9] C. Alexandrou, K. Cichy, M. Constantinou, K. Hadjiyiannakou, K. Jansen, H. Panagopoulos, and F. Steffens, *A complete non-perturbative renormalization prescription for quasi-PDFs*, *Nucl. Phys.* **B923** (2017) 394–415, [arXiv:1706.00265].

[10] Y.-S. Liu, W. Wang, J. Xu, Q.-A. Zhang, J.-H. Zhang, S. Zhao, and Y. Zhao, *Matching Quasi Generalized Parton Distributions in the RI/MOM scheme*, `arXiv:1902.00307`.

[11] The Nuclear Science Advisory Committee's October 2015 Long Range Plan for Nuclear Science *Reaching for the Horizon.*

[12] N. A. of Sciences Engineering Medicine, *An Assessment of U.S.-Based Electron-Ion Collider Science.* 2018.

[13] M. Constantinou, *Renormalization Issues on Long-Link Operators*, in *7th Workshop of the APS Topical Group on Hadronic Physics*, Feb 1-3, 2017.

[14] J.-W. Chen, T. Ishikawa, L. Jin, H.-W. Lin, Y.-B. Yang, J.-H. Zhang, and Y. Zhao, *Parton distribution function with nonperturbative renormalization from lattice QCD*, *Phys. Rev.* **D97** (2018), no. 1 014505, [`arXiv:1706.01295`].

[15] **LP3** Collaboration, H.-W. Lin, J.-W. Chen, T. Ishikawa, and J.-H. Zhang, *Improved parton distribution functions at the physical pion mass*, *Phys. Rev.* **D98** (2018), no. 5 054504, [`arXiv:1708.05301`].

[16] J.-W. Chen, L. Jin, H.-W. Lin, Y.-S. Liu, Y.-B. Yang, J.-H. Zhang, and Y. Zhao, *Lattice Calculation of Parton Distribution Function from LaMET at Physical Pion Mass with Large Nucleon Momentum*, `arXiv:1803.04393`.

[17] H.-W. Lin, J.-W. Chen, L. Jin, Y.-S. Liu, Y.-B. Yang, J.-H. Zhang, and Y. Zhao, *Spin-Dependent Parton Distribution Function with Large Momentum at Physical Pion Mass*, `arXiv:1807.07431`.

[18] Y.-S. Liu, J.-W. Chen, L. Jin, R. Li, H.-W. Lin, Y.-B. Yang, J.-H. Zhang, and Y. Zhao, *Nucleon Transversity Distribution at the Physical Pion Mass from Lattice QCD*, `arXiv:1810.05043`.

[19] X. Ji, A. Schäfer, X. Xiong, and J.-H. Zhang, *One-Loop Matching for Generalized Parton Distributions*, *Phys. Rev.* **D92** (2015) 014039, [`arXiv:1506.00248`].

[20] X. Xiong and J.-H. Zhang, *One-loop matching for transversity generalized parton distribution*, *Phys. Rev.* **D92** (2015), no. 5 054037, [`arXiv:1509.08016`].

[21] C. Alexandrou, K. Cichy, M. Constantinou, K. Hadjiyiannakou, K. Jansen, F. Steffens, and C. Wiese, *New Lattice Results for Parton Distributions*, `arXiv:1610.03689`.

[22] R. Frezzotti and G. C. Rossi, *Chirally improving Wilson fermions. 1. O(a) improvement*, *JHEP* **08** (2004) 007, [`hep-lat/0306014`].

[23] **ETM** Collaboration, A. Abdel-Rehim et al., *Simulating QCD at the Physical Point with Nf=2 Wilson Twisted Mass Fermions at Maximal Twist*, `arXiv:1507.05068`.

[24] **ETM** Collaboration, A. Abdel-Rehim, C. Alexandrou, M. Constantinou, K. Hadjiyiannakou, K. Jansen, C. Kallidonis, G. Koutsou, and A. Vaquero Aviles-Casco, *Direct Evaluation of the Quark Content of Nucleons from Lattice QCD at the Physical Point*, *Phys. Rev. Lett.* **116** (2016), no. 25 252001, [`arXiv:1601.01624`].

[25] C. Alexandrou, M. Constantinou, K. Hadjiyiannakou, K. Jansen, C. Kallidonis, G. Koutsou, A. Vaquero AvilÃ©s-Casco, and C. Wiese, *Nucleon Spin and Momentum Decomposition Using Lattice QCD Simulations*, *Phys. Rev. Lett.* **119** (2017), no. 14 142002, [`arXiv:1706.02973`].

[26] C. Alexandrou, K. Cichy, M. Constantinou, K. Hadjiyiannakou, K. Jansen, A. Scapellato, and F. Steffens, *Systematic uncertainties in parton distribution functions from lattice QCD simulations at the physical point*, `arXiv:1902.00587`.

[27] S. Alekhin, J. Blümlein, S. Moch, and R. Placakyte, *Parton distribution functions, α_s, and heavy-quark masses for LHC Run II*, *Phys. Rev.* **D96** (2017), no. 1 014011, [`arXiv:1701.05838`].

[28] **NNPDF** Collaboration, R. D. Ball et al., *Parton distributions from high-precision collider data*, *Eur. Phys. J.* **C77** (2017), no. 10 663, [`arXiv:1706.00428`].

[29] A. Accardi, L. T. Brady, W. Melnitchouk, J. F. Owens, and N. Sato, *Constraints on large-x parton distributions from new weak boson production and deep-inelastic scattering data*, *Phys. Rev.* **D93** (2016), no. 11 114017, [`arXiv:1602.03154`].

[30] D. de Florian, R. Sassot, M. Stratmann, and W. Vogelsang, *Extraction of Spin-Dependent Parton Densities and Their Uncertainties*, *Phys. Rev.* **D80** (2009) 034030, [`arXiv:0904.3821`].

[31] **NNPDF** Collaboration, E. R. Nocera, R. D. Ball, S. Forte, G. Ridolfi, and J. Rojo, *A first unbiased global determination of polarized PDFs and their uncertainties*, *Nucl. Phys.* **B887** (2014) 276–308, [`arXiv:1406.5539`].

[32] J. J. Ethier, N. Sato, and W. Melnitchouk, *First simultaneous extraction of spin-dependent parton distributions and fragmentation functions from a global QCD analysis*, *Phys. Rev. Lett.* **119** (2017), no. 13 132001, [`arXiv:1705.05889`].

[33] H.-W. Lin, W. Melnitchouk, A. Prokudin, N. Sato, and H. Shows, *First Monte Carlo Global Analysis of Nucleon Transversity with Lattice QCD Constraints*, *Phys. Rev. Lett.* **120** (2018), no. 15 152502, [`arXiv:1710.09858`].

[34] J.-W. Chen, S. D. Cohen, X. Ji, H.-W. Lin, and J.-H. Zhang, *Nucleon Helicity and Transversity Parton Distributions from Lattice QCD*, *Nucl. Phys.* **B911** (2016) 246–273, [`arXiv:1603.06664`].

[35] G. S. Bali, B. Lang, B. U. Musch, and A. SchÃ¤fer, *Novel quark smearing for hadrons with high momenta in lattice QCD*, *Phys. Rev.* **D93** (2016), no. 9 094515, [`arXiv:1602.05525`].

[36] A. Frommer, K. Kahl, S. Krieg, B. Leder, and M. Rottmann, *Adaptive Aggregation Based Domain Decomposition Multigrid for the Lattice Wilson Dirac Operator*, *SIAM J. Sci. Comput.* **36** (2014) A1581–A1608, [`arXiv:1303.1377`].

[37] M. Luscher, *Solution of the Dirac equation in lattice QCD using a domain decomposition method*, *Comput. Phys. Commun.* **156** (2004) 209–220, [`hep-lat/0310048`].

[38] M. Luscher, *Local coherence and deflation of the low quark modes in lattice QCD*, *JHEP* **07** (2007) 081, [`arXiv:0706.2298`].

[39] C. Alexandrou, S. Bacchio, J. Finkenrath, A. Frommer, K. Kahl, and M. Rottmann, *Adaptive Aggregation-based Domain Decomposition Multigrid for Twisted Mass Fermions*, *Phys. Rev.* **D94** (2016), no. 11 114509, [`arXiv:1610.02370`].

[40] C. Alexandrou, S. Gusken, F. Jegerlehner, K. Schilling, and R. Sommer, *The Static approximation of heavy - light quark systems: A Systematic lattice study*, *Nucl. Phys.* **B414** (1994) 815–855, [`hep-lat/9211042`].

[41] S. Gusken, *A Study of smearing techniques for hadron correlation functions*, *Nucl. Phys. Proc. Suppl.* **17** (1990) 361–364.